A nano-fibrous assembly of collagen–hyaluronic acid for controlling cell-adhesive properties†

Toshinori Fujie,[a] Sho Furutate,[a] Daisuke Niwa[a] and Shinji Takeoka*[ab]

Received 14th June 2010, Accepted 15th July 2010
DOI: 10.1039/c0sm00527d

We report an artificially fabricated extracellular matrix (ECM)-like nanostructure, which utilizes self-assembly of collagen and hyaluronic acid in a quasi two-dimensional space of tens-of-nm thickness, displaying different cellular adhesive characteristics depending on the structural properties between the fibril and non-fibril elements. This nano-fibrous assembly will facilitate a mechano-biological approach for the development of tissue-engineering scaffolds.

An extracellular matrix (ECM) is composed of structural proteins (*e.g.*, collagen (COL), laminin, fibronectin, vitronectin, elastin), signaling proteins (*e.g.*, growth factors, small multicellular proteins, small integrin-binding glycoproteins) and proteoglycans (*e.g.*, hyaluronic acid (HA) and chondroitin sulfate).[1] Several attempts have been made to fabricate ECM-like structures with regard to their biological, chemical and mechanical properties.[2–4] These studies have generally been undertaken on solid substrates such as plastic, glass or silicon wafers. Recently, an alternative approach focusing on the mechanical properties of the substrates towards cellular activities has been developed using soft materials such as elastic gels and rubbers. This strategy is particularly attractive because the mechanical properties of the substrate can be easily tuned by changing the crosslinking density or the composition of the material.[5,6] Nonetheless, properties of the substrate (physical, chemical and mechanical) have not yet been fully explored in relation to the cell cycle in a living body. In this study, we directly focus on the structure of the ECM, specifically the fibrous assembly derived from biopolymers of type I COL and HA, with regard to its mechanical characteristics and the corresponding effect on cellular properties. As far as we know, this is the first report demonstrating such morphological control of cellular behavior using a freestanding ECM derived ultra-thin film (*i.e.*, ECM-nanosheets) fabricated by non-covalent molecular assembly.

Fabrication of the freestanding polymer nanosheet was carried out in combination with a supporting film and the entire process was undertaken in an aqueous medium.[7,8] The multilayer of COL and HA on the solid substrate was prepared using a layer-by-layer (LbL) assembly method.[9–11] Both layers of COL and HA were prepared from the corresponding acetate buffer solutions (pH 4.7, 0.5 mg/mL), which induced a stable electrostatic interaction between each layer. The 7.5 pairs of COL and HA layers were then assembled on a SiO_2 substrate (Fig. S1, ESI†). The resulting multilayered COL/HA film was peeled from the SiO_2 substrate by means of a supporting film method.[7,8] This approach allows collection of the freestanding polymer nanosheet by dissolving away the water-soluble supporting film (70 μm thick), which is composed of poly(vinyl alcohol) (PVA), leaving the multilayered COL/HA nanosheet (62 nm thick) intact (Fig. S2, ESI†). Because the interaction between the bilayered components is greater than that between the COL/HA nanosheet and the SiO_2 substrate, the bilayered film can be separated from the edge of the SiO_2 substrate with tweezers prior to dissolving the PVA film in water to release a freestanding nanosheet.[7] This methodology is suitable for collection of a protein-containing polymer nanosheet because the procedure does not require any organic solvents, which might induce denaturation of the protein component(s) (*e.g.*, collagen).

The thickness of the ECM-nanosheets and their surface morphology were analyzed using a surface profiler, which involved transferring the freestanding nanosheet in water onto a silicon wafer. The thickness of the ECM-nanosheet increased exponentially as a function of the number of COL and HA layer pairs (Fig. 1a). One reason for this exponential growth is that the amount of hyaluronan adsorbed in the LbL structure is less than that of COL.[12] In fact, HA forms networks composed of double stranded helices with molecular dimensions of approximately 0.5 nm.[13] However, COL has larger molecular dimensions, such that its smallest structural unit is the microfibril with a width of approximately 1.5–4 nm and a length of 300–500 nm.[13,14] Therefore, the polyion pairs mediated by the electrostatic interaction between COL and HA molecules induce non-linear growth in the LbL system.

By using a water-soluble supporting film, the ECM-nanosheet can also be transferred onto various interfaces such as an air–water interface (Fig. 1b), skin (Fig. 1c) or polystyrene Petri-dish (Fig. 1d). In particular, the original ECM-nanosheet, which is the same shape as the substrate, can be cut into the desired shape (Fig. 1d). This useful property allows the shape and size of cell adhesive region to be readily controlled, where NIH-3T3 cells were then transferred onto the ECM-nanosheet. Next, we confirmed that the cells had specifically adhered to the region of the ECM-nanosheet and not to the intact polystyrene surface (Fig. 1e). Moreover, the magnified images revealed that the individual pseudopodia of the cells on the ECM-nanosheet had integrated into the region of the ECM-nanosheet (Fig. 1f). Therefore, the ECM-nanosheet conveniently generated a more cytophilic surface than the conventional polystyrene surface.

One of the characteristic features of the natural ECM is a fibril structure of COL, which was produced thermodynamically in this study by incubating the prepared ECM-nanosheet in the physiological conditions using a phosphate buffer saline (PBS) at 37 °C (see ESI†). The microscopic surface morphology of the 65 nm thick ECM-nanosheet (7.5 layer pairs) shows a plethora of microfibrils originating from the COL and HA complex (see AFM image in

[a]*Department of Life Science and Medical Bioscience, Graduate School of Advanced Science and Engineering, Waseda University, 2-2 Wakamatsu-cho, Shinjuku-ku, Tokyo, 162-8480, Japan. E-mail: takeoka@waseda.jp; Fax: +813-5369-7324; Tel: +813-5369-7324*
[b]*High-Tech Research Center, Waseda University, Tokyo, 162-8480, Japan*
† Electronic supplementary information (ESI) available: Preparative scheme of the ECM-nanosheet. See DOI: 10.1039/c0sm00527d

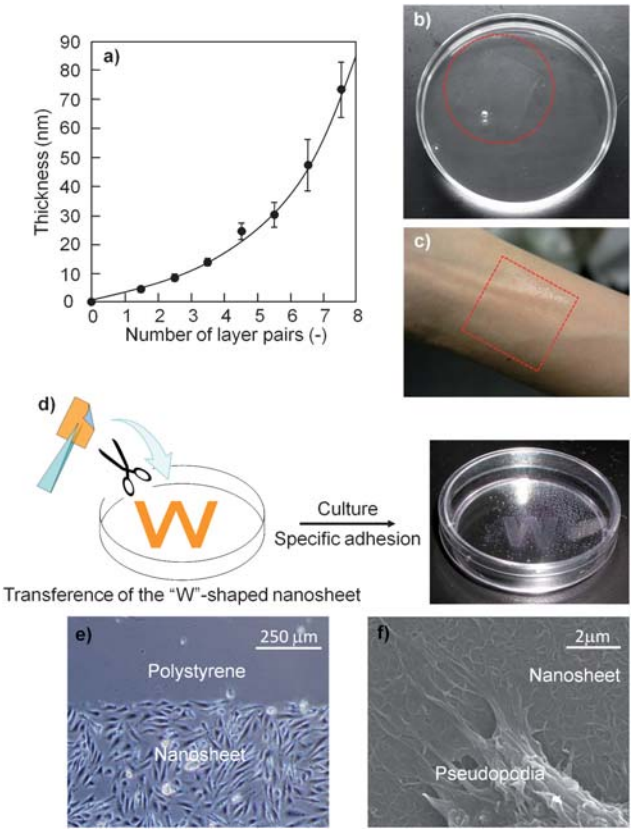

Fig. 1 Transfer of the ECM-nanosheet onto various surfaces. (a) Thickness of the ECM-nanosheets measured by a surface profiler as a function of the number of COL and HA layer pairs. Macroscopic image of the ECM-nanosheets transferred onto the various surfaces: (b) air–water interface, (c) human skin and (d) specific area of a Petri-dish, on which cells (NIH-3T3) grew. (e) Magnified image of the edge in (d) between the ECM-nanosheet and the intact Petri-dish. (f) SEM image of the cellular pseudopodia adhering to the ECM-nanosheet.

Fig. 2a and c). The microfibrils were less than 0.2 μm in width and approximately 10 μm in length, as estimated from a SEM image (Fig. 2a, arrows). However, several large fibrils over 100 μm in length were observed after incubation of the ECM-nanosheet in PBS (pH 7.4) at 37 °C (Fig. 2b, arrows and d). Importantly, the magnified SEM image of the individual long fibrils showed a periodic structure of approximately 67 nm (Fig. 2e), indicating the formation of COL fibrils.[15] Based on the SEM images, we confirmed the surface coverage of the longitudinal COL fibrils. Specifically, we clarified that the COL fibrils display 50% surface coverage within 12 h (Fig. 2f). By monitoring the fluorescent-labeled HA, we established that ~56% of the HA in the ECM-nanosheet dissociated after only 2 h incubation (see Fig. S3, ESI†). This observation suggests that dissociation of HA under physiological conditions triggers the thermodynamic self-assembly of COL molecules into the long fibril assembling state. Considering the pK_a of HA (around 4.7), the physiological conditions of pH 7.4 and 37 °C enhances deprotonation of the carboxylic acids of HA and renders HA soluble in PBS. At the same time, deprotonation of the positively charged amines occurs in COL at pH 7.4, leading to the disassembly of COL–HA complexes. Thus, the self-assembly process is driven by the fact that the remaining COL molecules no longer possess a counter polyanion of HA in the ECM-nanosheet, resulting in the COL fibrilization by hydrophobic interaction. Hence, depending on their COL structures we can distinguish the ECM-nanosheets into two distinct types. One type represents the fibril (F) nanosheets, obtained after 12 h incubation under physiological conditions (PBS, 37 °C). By contrast, the non-fibril (NF) nanosheets comprise intact COL–HA fibrils generated by the LbL method.

We used a bulge test[16] to evaluate the mechanical strength of the various ECM-nanosheets. The F- and NF-nanosheets with a thickness of 42 and 62 nm, respectively, were transferred to physically cover a 6 mm diameter circular hole in a stainless steel plate.[7] The mounted ECM-nanosheet was then placed in a custom-made chamber, where air pressure was applied through the circular hole until distortion of the nanosheet was observed. Ambient conditions (*i.e.*, temperature: 25 °C, humidity: 37%) were maintained during the bulge test. The relationship between pressure and deflection was found to be non-linear and the overall deflection of both ECM-nanosheets was damped by an increase in thickness (Fig. 3a). Interestingly, the deflection of NF-nanosheets (Fig. 3b) was larger than that of the F-nanosheets (Fig. 3c), suggesting that the COL fibrils provide stiffness to the F-nanosheet. Therefore, we converted the pressure–deflection curve into a stress–strain curve to estimate the elastic modulus of both nanosheets (Fig. 3d). From the initial elasticity of the stress–strain curve, the ultimate tensile strength (σ_{max}), elongation (ε_{max}) and elastic modulus (E) were calculated for the F (F-nanosheets) and NF (NF-nanosheets) types of the ECM-nanosheets (Table 1).

The elastic modulus of the NF-nanosheet (62 nm thick) was 4.3 ± 0.6 GPa, which is a comparably smaller value than that of the previously reported polysaccharide nanosheet (E = 9.6 GPa, 75 nm thick composed of chitosan and alginate)[7] as well as the silk fibroin nanosheet (E = 6–8 GPa, less than 100 nm thick).[17] The very low elastic modulus of the NF-nanosheet is presumably derived from the hydrophilic and moisture-sensitive nature of the HA molecules. In fact, the water contact angle of the NF-nanosheets (40 ± 7 degrees) is lower than that of the chitosan–alginate nanosheets (62 degrees). However, the elastic modulus of the F-nanosheet (42 nm thick) was 12.5 ± 1.5 GPa, which gives three-fold greater mechanical durability than the NF-nanosheet, despite the thickness of the F-nanosheet being slightly reduced due to dissociation of HA molecules (*i.e.*, ~56% of the HA molecules were dissociated in the F-nanosheet by comparison with the original ECM-nanosheet). Considering the higher ultimate tensile strength of the F-nanosheets (289 ± 9 MPa) over the NF-nanosheets (227 ± 10 MPa), the ECM-nanosheets should be reinforced by the self-assembled fibrous structure of the COL molecules. Such mechanical enhancement by incorporating the nanofibers in the LbL film was demonstrated by Kotov and co-workers, where single walled carbon nanotubes in the LbL film reinforced its mechanical properties.[18] Therefore, COL fibrils in this study should also reinforce the nanosheet. Moreover, natural COL structures also show a range of different mechanical properties.[19] For example, most COL structures in bone have an elastic modulus of 17.2 GPa (close to that of F-nanosheets), whereas those of skin have an elastic modulus of 4 GPa (close to that of NF-nanosheets). Hence, we succeeded in enhancing the mechanical strength by changing the self-assembled structure of the COL molecules inside of the quasi two-dimensional planar surface. Thus, the F-nanosheets imitated the COL matrices around the bone and the NF-nanosheets imitated those around the skin.

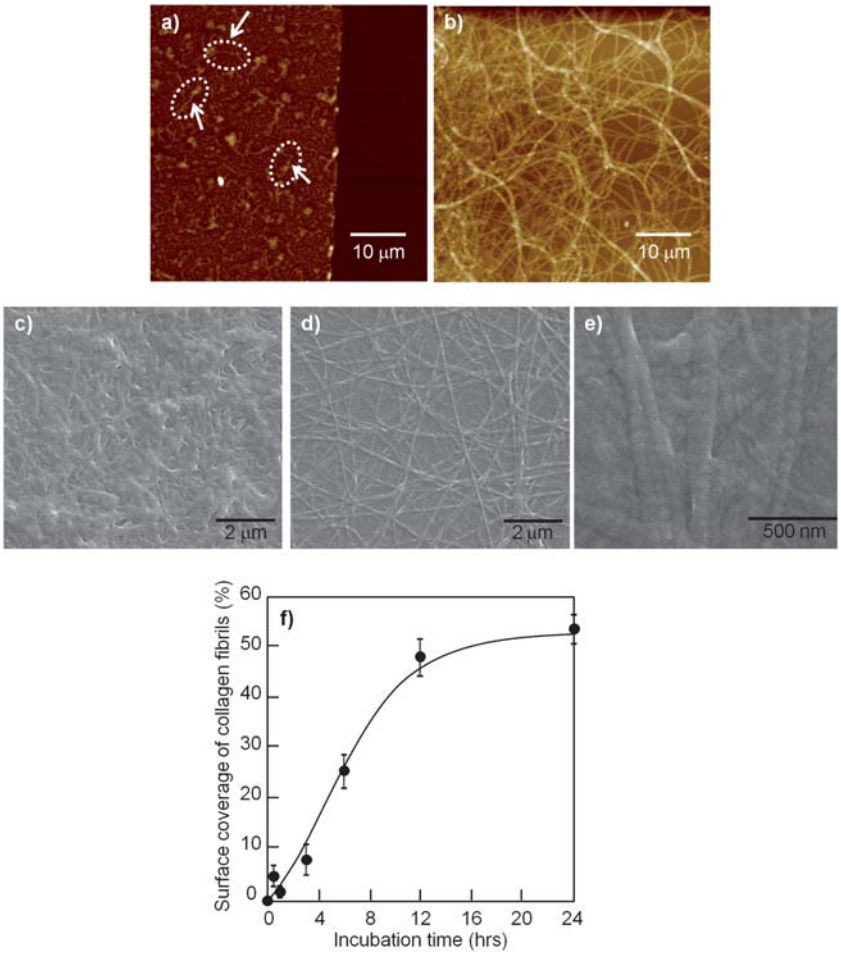

Fig. 2 Generation of COL fibrils in the ECM-nanosheet. AFM and SEM images of (a), (c) NF-nanosheet and (b), (d) F-nanosheet. Magnified image of COL fibrils in (d); a periodic structure (*ca.* 67 nm) of the COL fibril was observed. (f) Surface coverage of COL fibrils, as determined from SEM images such as (d).

Next, we focused on the mechanical effects of the ECM-nanosheets (F- and NF-nanosheets) on cell adhesive properties. The nanosheet was scooped onto a stainless steel mesh with a 0.6 mm × 0.6 mm lattice (Fig. S2, ESI†). Cell adhesive morphology was then statistically evaluated by integration of the individual cell behavior. Immunostaining of the cellular cytoskeleton, such as actin filaments (red by phalloidin) and the nucleus (blue by DAPI), showed a remarkable difference in the adhesive morphology between F and NF-nanosheets (green by FITC) after at least 4 h incubation. Cells on the NF-nanosheet heterogeneously tethered along the frames of the stainless steel mesh (Fig. 4a) without spreading pseudopodia (Fig. 4b). Indeed, the image of an individual cell (Fig. 4a) was colored purple (*i.e.*, merged color of red (actin) and blue (nucleus)), indicating a stagnation of pseudopodial spreading. By contrast, cells on the F-nanosheet homogeneously adhered to the surface (Fig. 4c). Images of individual cells were colored red (*i.e.*, enhanced image of actin) suggesting typical pseudopodial spreading. Moreover, the magnified image of the F-nanosheet displayed partial corrugation of the nanosheet corresponding to a contraction of the cells (Fig. 4d, arrows). Separate microscopic images verified that the F-nanosheet adopted a corrugated surface due to contracted cells (Fig. S4, ESI†). These observations are consistent with a past report, which demonstrated that fibroblast locomotion and contractibility of cells causes a visible wrinkling of a silicone rubber substrate upon crawling.[20] In addition to the adhesive behavior, the pseudopodial elongation of the cells was observed along with the direction of the COL fibril extension in the case of the F-nanosheets (data not shown). However, such elongation of the cell was not significantly observed on the overall surface texture of F-nanosheet because each COL fibril did not orientate to enhance the polarization of the cells but randomly located as shown in Fig. 1d. Hence, individual cells would recognize the structural differences of the overall surface texture between F- and NF-nanosheets rather than the direction of the COL fibrils. Besides, these results also suggested that the importance of the tens-of-nm thickness. The past paper reported by Picart and co-workers[14] evaluated the change of the surface texture of the COL–HA multilayered films along the increment of thickness up to μm of the bulk scale, where the large fibril structure was enhanced to be formed by gradual assembly of COL molecules into the fibril states; the cell adhesive properties showed the same level as the F-nanosheets. These results suggested that the bulk materials composed of COL–HA produced the fibril texture, while the methodology was not adopted to control the cell adhesive properties in the comparison with the present study. Hence, it is important to use the

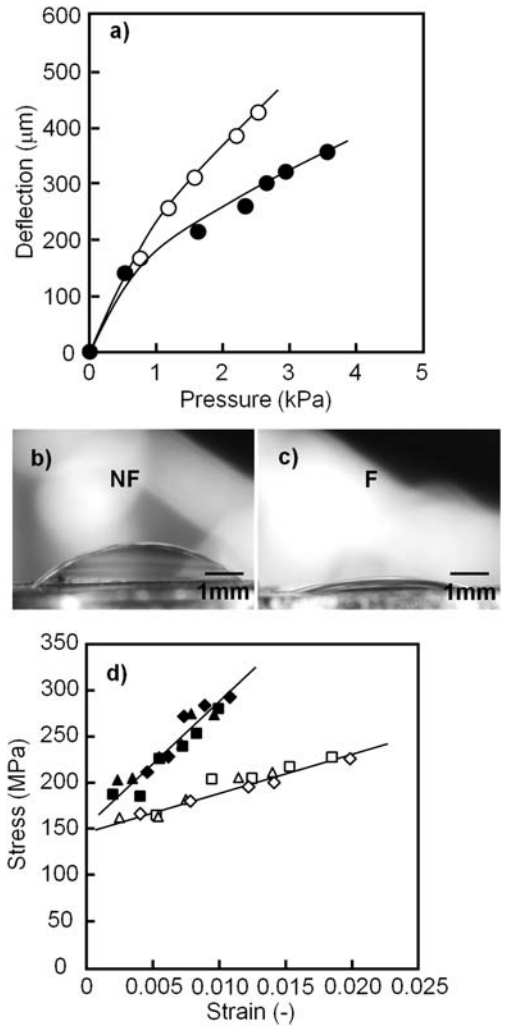

Fig. 3 Mechanical properties of the ECM-nanosheets. (a), Pressure–deflection curve and (d) stress–strain curve of NF (blank symbols) and F (solid symbols)-nanosheets. For example, each symbol (◆, ■ or ▲) in (d) represents different experimental data using the F-nanosheet. (b), (c) Cross-sectional images of deflected ECM-nanosheets.

Table 1 Mechanical properties of ECM-nanosheets with or without collagen fibers

Structure	Thickness: h (nm)	Ultimate tensile strength: σ_{max} (MPa)	Ultimate tensile elongation: ε_{max} (%)	Elastic modulus: E (GPa)
F	42 ± 4.4	289 ± 9	1.0 ± 0.1	12.5 ± 1.5
NF	62 ± 7.4	227 ± 10	1.7 ± 0.3	4.3 ± 0.6

nanosheet for the preparation of different surface textures as well as different cell adhesive properties because such differences can be produced by the thermodynamic assembly of COL and HA molecules in the quasi two-dimensional interface.

During the adhesion process, NIH-3T3 cells elongate or become polarized. Further details of the cell adhesive property was investigated by the cell elongation ratio at 24 h using the following formula:[21]

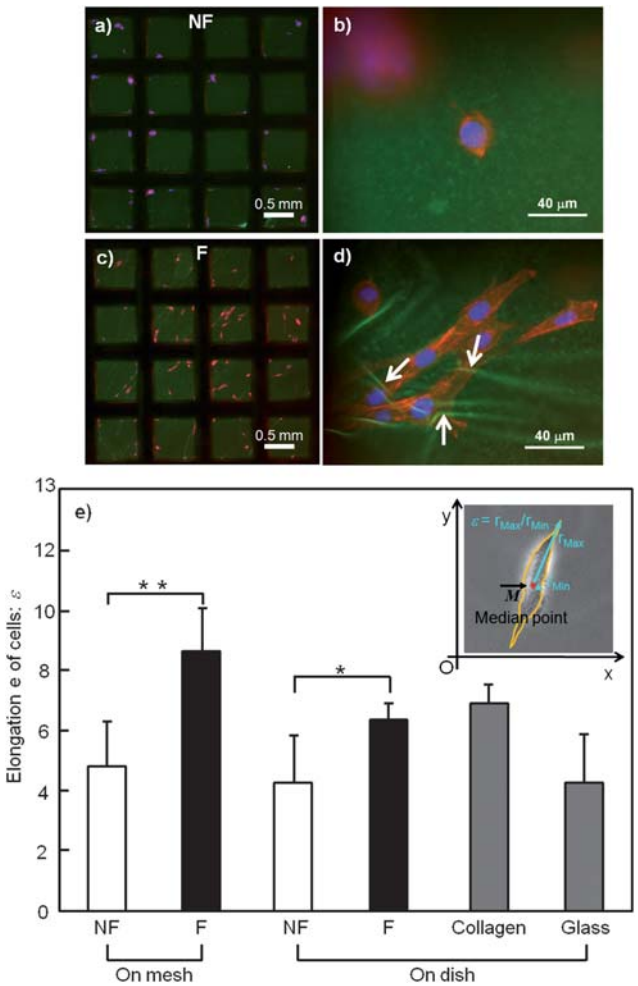

Fig. 4 Cell adhesive characteristics of ECM-nanosheets displaying different mechanical properties. NIH-3T3 cells after 4 h on the NF (a) or F (c)-nanosheets suspended on a stainless steel mesh. Cells were stained with phalloidin (red) and DAPI (blue). Panels (b) and (d), correspond to magnified images of panels (a) and (c), respectively. Arrows highlight corrugation of the F-nanosheet. (e) Cell elongation ratio for NIH-3T3 cells adhered to the F (solid bar) or NF-nanosheet (blank bar) on the stainless steel mesh or the glass-bottomed dish for 24 h. Statistical significance by the ANOVA test (N = 3) were set as $^{**}p < 0.01$ and $^{*}p < 0.05$, respectively. As positive and negative control samples, collagen-coated glass and intact glass-bottomed dish (shaded bar) were also used.

$$\varepsilon = r_{max}/r_{min}$$

where ε represents the cell elongation ratio and r_{max}, r_{min} represents the maximum and minimum distances of pseudopodia adhered from the median point of the cell, respectively (Fig. 4e). The F-nanosheet on the dish (glass-bottom dish) as well as collagen-coated glass allowed cells to elongate slightly more than the NF-nanosheets and the intact glass-bottom dish. In particular, the F-nanosheets significantly enhanced the elongation in comparison with the NF-nanosheets ($^{*}p < 0.05$). We assume that integrin molecules are prevented from binding to collagen microfibrils by steric-repulsion of the surrounding swollen HA molecules in the NF-nanosheets.[14] Indeed, the cytoskeleton (actin filaments) did not propagate as shown in the immunostaining image in Fig. 4a. By contrast, cells on the

F-nanosheet mesh elongated significantly more than the NF-nanosheet mesh (**$p < 0.01$) and this difference was already evident after the 4 h culture (Fig. S5, ESI†). Moreover, the F-nanosheets on the mesh enhanced the elongation ratio compared with that on the dish, whereas the NF-nanosheets gave similar levels of cell elongation ratio between mesh and dish. Thus, enhancement in the cell elongation ratio on the F-nanosheet can be explained by the presence of COL fibrils as the following mechanisms: (1) a decrease in the amount of HA molecules in the nanosheet suppresses HA-related repulsive force and enhances ligand–receptor binding between COL and cellular integrin, and (2) an increment in the mechanical stiffness of the ECM-nanosheet induces tighter association of the cells. This mechanical stiffness particularly enhances the focal adhesion of the cells on the nanosheet such as actin polymerization, which is sequentially continued from the cellular tethering behavior in process (1). This second point is also supported by a previous report, which suggested that matrix stiffness modulates cell morphology during the process of adhesion or differentiation.[5]

In summary, we have fabricated two kinds of freestanding ECM-nanosheets by thermodynamically controlling the amount of COL and HA. The F-nanosheets possessed the COL fibril structures and had a low content of HA molecules, which enhanced both the mechanical stiffness of the surface and adhesive elongation of the cells. The NF-nanosheets possessed non-COL fibrils and a high content of HA molecules, which imparted a surface with soft elastic properties and gave lower adhesive elongation of the cells. On the basis of the present study, cell adhesive properties can be tuned by changing the structural components of the ECM-nanosheets, such as the content of HA and COL fibrils. In future, the effect of including additional ECM components, such as signaling proteins, on the properties of the ECM-nanosheet will be explored. Such an approach will generate a more natural ECM, which will open new avenues of research for the production of novel engineered scaffolds for regenerative medicine as well as cell biology.

Acknowledgements

The authors thank Assoc. Prof. Teruyuki Komatsu at the Research Institute for Science & Engineering, Waseda University for technical advice and useful discussions concerning the SEM observations. This work was supported in part by "High-Tech Research Center" Project for Waseda University: matching fund subsidy (S.T.) from MEXT; grant-in-aid for Scientific Research (B) 21300181 from MEXT (S.T.); Cooperative program for Graduate Student Education with University of Yamanashi from MEXT, Japan (T.F. and S.T.); Adaptable and Seamless Technology Transfer Program through Target-driven R&D (A-STEP) from JST, Japan (T.F. and S.T.).

References

1 H. Fernandes, L. Moroni, C. van Blitterswijk and J. de Boer, *J. Mater. Chem.*, 2009, **19**, 5474.
2 Z. Tang, Y. Wang, P. Podsiadlo and N. A. Kotov, *Adv. Mater.*, 2006, **18**, 3203.
3 K. Ren, T. Crouzier, C. Roy and C. Picart, *Adv. Funct. Mater.*, 2008, **18**, 1378.
4 C. J. Bettinger, R. Langer and J. T. Borenstein, *Angew. Chem., Int. Ed.*, 2009, **48**, 5406.
5 A. J. Engler, S. Sen, H. L. Sweeney and D. E. Discher, *Cell*, 2006, **126**, 677.
6 D. E. Discher, P. Janmey and Y.-L. Wang, *Science*, 2005, **310**, 1139.
7 T. Fujie, N. Matsutani, M. Kinoshita, Y. Okamura, A. Saito and S. Takeoka, *Adv. Funct. Mater.*, 2009, **19**, 2560. and also see*Nature Nanotech.* 2009, 4, 472.
8 T. Fujie, J.-Y. Park, A. Murata, N. C. Estillore, M. C. R. Tria, S. Takeoka and R. C. Advincula, *ACS Appl. Mater. Interfaces*, 2009, **1**, 1404.
9 G. Decher, J. B. Schlenhoff (Eds), in *Multilayer Thin Films: Sequential Asssembly of Nanocompsoite Materials*, Wiley-VCH, 2003, Weinheim.
10 C. Jiang and V. V. Tsukruk, *Adv. Mater.*, 2006, **18**, 829.
11 K. Ariga, J. P. Hill and Q. Ji, *Phys. Chem. Chem. Phys.*, 2007, **9**, 2319.
12 C. Picart, J. Mutterer, L. Richert, Y. Luo, G. D. Prestwich, P. Schaaf, J.-C. Voegel and P. Lavalle, *Proc. Natl. Acad. Sci. U. S. A.*, 2002, **99**, 12531.
13 J. A. Johansson, T. Halthur, M. Herranen, L. Söderberg, U. Elofsson and J. Hilborn, *Biomacromolecules*, 2005, **6**, 1353.
14 J. Zhang, B. Senger, D. Vautier, C. Picart, P. Schaaf, J.-C. Voegel and P. Lavalle, *Biomaterials*, 2005, **26**, 3353.
15 M. J. Buehler and Y. C. Yung, *Nat. Mater.*, 2009, **8**, 175.
16 C. Jiang, S. Markutsya, Y. Pikus and V. V. Tsukruk, *Nat. Mater.*, 2004, **3**, 721.
17 C. Jiang, X. Wang, R. Gunawidjaja, Y.-H. Lin, M. K. Gupta, D. L. Kaplan, R. R. Naik and V. V. Tsukruk, *Adv. Funct. Mater.*, 2007, **17**, 2229.
18 A. A. Mamedov, N. A. Kotov, M. Prato, D. M. Guldi, J. P. Wicksted and A. Hirsch, *Nat. Mater.*, 2002, **1**, 190.
19 C. R. Carlisle, C. Coulais and M. Guthold, *Acta Biomater.*, 2010, **6**, 2997.
20 A. K. Harris, P. Wild and D. Stopak, *Science*, 1980, **208**, 177.
21 M. J. Dalby, N. Gadegaard, R. Tare, A. Andar, M. O. Riehle, P. Herzyk, C. D. W. Wilkinson and R. O. C. Oreffo, *Nat. Mater.*, 2007, **6**, 997.

